Anisotropy of the critical temperature of a superconducting niobium thin film with an array of nanoscale holes in an external magnetic field

M. L. Latimer, Z. L. Xiao, J. Hua, A. Joshi-Imre, Y. L. Wang, R. Divan, W. K. Kwok, and G. W. Crabtree

Phys. Rev. B **87**, 020507 — Published 22 January 2013

DOI: 10.1103/PhysRevB.87.020507

Anisotropy of the Critical Temperature of a Superconducting Niobium Thin Film with an Array of Nanoscale Holes in an External Magnetic Field

M. L. Latimer[1,2], Z. L. Xiao[1,2,*] J. Hua[3], A. Joshi-Imre[4], Y. L. Wang[1], R. Divan[4], W. K. Kwok[1], and G. W. Crabtree[1,5]

[1]*Materials Science Division, Argonne National Laboratory, Argonne, Illinois 60439*
[2]*Department of Physics, Northern Illinois University, DeKalb, Illinois 60115*
[3]*Nebraska Center for Materials and Nanoscience, Lincoln, Nebraska 68588*
[4]*Center for Nanoscale Materials, Argonne National Laboratory, Argonne, Illinois 60439 and*
[5]*Departments of Physics, Electrical and Mechanical Engineering, University of Illinois at Chicago, Illinois 60607*

(Dated: January 14, 2013)

We report on magneto-transport experiments investigating the effect of a regular array of nanoscale holes on the anisotropic response in the transition temperature of a superconducting niobium thin film. We find that the angle dependence of the critical temperature exhibits two strong anisotropic effects: Little-Parks oscillations whose period varies with field direction and a smooth background arising from one-dimensional confinement by the finite lateral space between neighboring holes. The two components of the anisotropy are intrinsically linked and appear in concert with one superimposed on top of the other.

PACS numbers: 74.78.-w, 74.81.Fa, 74.25.Op

When the dimensions of a material are reduced to a characteristic length, new behavior emerges governed by a new set of mechanisms due to confinement-induced changes in the wave function of the charge carriers and other fundamental quantities[1–10]. For example, the circulation of Cooper pairs confined in a path with lateral dimensions comparable to the superconducting coherence length ξ produces the Little-Parks effect[1,8–13]. A superconducting strip narrower than its penetration depth λ cannot sustain a complete flux exclusion, resulting in lower diamagnetic energy which then leads to a higher critical field H_c[14,15]. An example is the parallel critical field $H_{c\parallel}$ of a superconducting thin film, whose value is increased by a factor of $2\sqrt{6}\lambda/t$ over its bulk value, where t is the film thickness[14,15]. Such confinement effects can imbue an isotropic non-spherical three-dimensional (3D) superconductor with anisotropic properties when its dimensions are reduced to the order of λ, as evidently demonstrated by the well-known Tinkham formula[15] $H_{c\theta}\cos\theta/H_{c\perp} + (H_{c\theta}\sin\theta/H_{c\parallel})^2 = 1$ for the angle dependent critical field $H_{c\theta}$ of a 2D superconducting film. Here, $H_{c\perp}$ is the critical field for the magnetic field perpendicular to the film surface and θ is the angle between the magnetic field and the normal to the film.

Superconducting films with arrays of nanoscale holes have been explored widely to enhance vortex pinning and hence the current carrying capability of superconductors[16–20]. More broadly, these nano-patterned superconducting films can also serve as model systems to study emergent phenomena that appear across many physical systems such as frustration and to explore the dynamics of driven periodic elastic media through an array of obstacles[21–25]. The two characteristic length scales in a superconductor, the coherence length, ξ, and the penetration depth, λ, become highly temperature dependent close to the zero-field critical temperature T_{c0}. Tuning the distances between neighboring holes in a superconducting film with a nano-patterned hole-array so that they are comparable to ξ or λ, creates a unique platform for exploring confinement-induced phenomena.

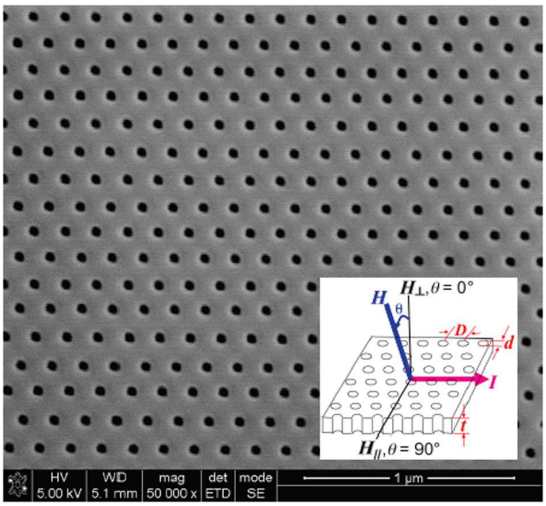

FIG. 1. (Color online) SEM micrograph of Sample A. The inset shows definitions of the magnetic field direction θ, film thickness t, and lattice constant D of the hole-array.

Here we present the first report on the anisotropy of the critical temperature T_c of a superconducting niobium film with a triangular hole lattice. We find a remarkably strong $T_c(\theta)$ anisotropy with magnetic field orientation, θ, that can be divided into two components: strong Little-Parks oscillations arising from the confinement of the Cooper pairs and a smooth background anisotropy that arises from incomplete flux exclusion in the regions between neighboring holes. Since the Little-Parks effect and the background anisotropy in $T_c(\theta)$ reveal that the lateral extent of superconducting sections between neighboring holes is quasi one-dimensional (1D), our results

TABLE I. Parameters of the patterned Nb films

Sample	D (nm)	d (nm)	t (nm)	T_{c0} (K)	$\xi(0)$ (nm)	$\alpha_\perp$ -Cal.	$\alpha_\perp$ -Exp.	T^* (K)
A	150	50	60	5.961	8.6	0.6	0.587	5.81
B	300	50	60	6.949	9.5	0.24	0.325	6.91

demonstrate that the hole-array can transform the characteristic of the film from 2D to 1D. This finding not only demonstrates a new paradigm of confinement-induced dimensionality change but it also directly impacts our previous understanding of phenomena reported in superconducting films with hole-arrays. For example, in experiments using hole-arrays as vortex pinning centers, one assumes that the dimensionality of the film is not affected by the hole-array, even though the transport measurements are conducted at temperatures near T_{c0}[26–28]. Our results may also shed light on the properties of other types of perforate structures where the confining hole geometry makes the width of the sections between neighboring holes comparable to the characteristic length scale of the investigated phenomena[29–34].

Niobium films (60 nm thick) with contacts for four-probe DC transport measurements were deposited onto silicon substrates with 200 nm thick oxide layers via DC magnetron sputtering. A triangular array of holes with diameter $d \approx 50$ nm was fabricated into the Nb film with focused-ion-beam (FIB) milling[35]. Two samples with hole-hole distances $D = 150$ nm (Sample A) and 300 nm (Sample B) were investigated using a constant current mode. A continuous film was also measured as a reference. Figure 1 shows a scanning electron microscopy (SEM) image of Sample A. The inset shows a schematic of the magnetic field and applied current geometry. The sample was placed on a stepper-controlled rotator with an angular resolution of 0.05°. The critical temperature T_c, was obtained from measurements of the temperature dependence of the resistance at fixed magnetic fields and field angles, using a criterion of $0.5R_N$ where R_N is the normal state resistance. Additional parameters for Samples A and B are presented in Table I.

The two panels in Fig.2 show $T_c(\theta)$ curves at various fixed magnetic fields for Samples A and B and represent the central experimental results of this study. Unlike the monotonic increase of that expected for a 2D continuous film as the magnetic field is away from the perpendicular orientation with respect to the film, the $T_c(\theta)$ of the patterned films show two dominant features: an oscillation with decreasing period in angle superimposed on a smooth increasing background. A quantitative comparison of Sample A and the reference film presented in the inset of Fig.2b for $T_c(\theta)$ curves obtained at 900 G shows that the $T_c(\theta)$ of the patterned film increases at a significantly slower rate when the field orientation approaches the parallel direction ($\theta = 90°$). This clearly shows that

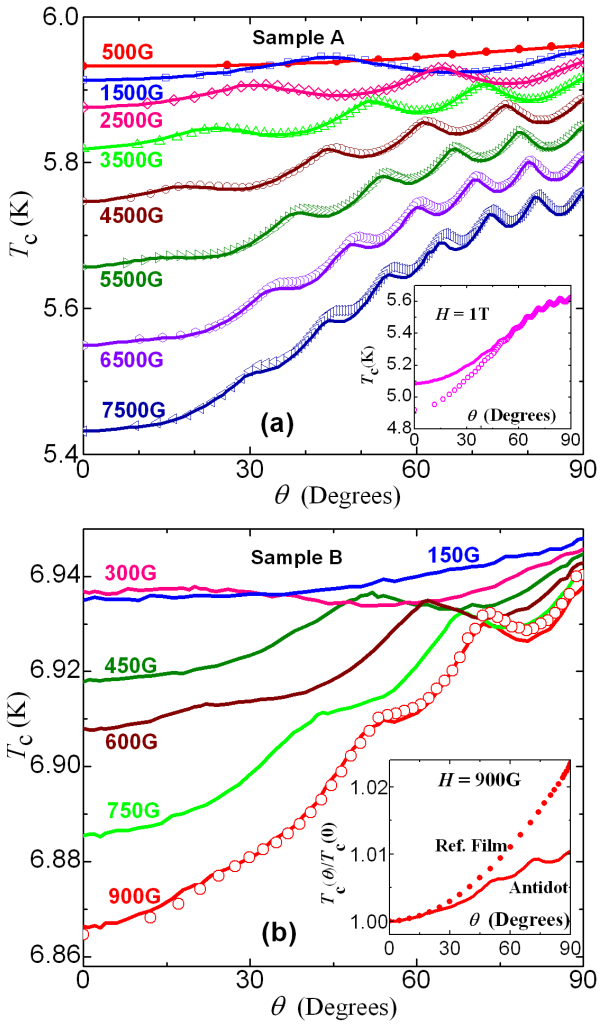

FIG. 2. (Color online) $T_c(\theta)$ obtained at various fixed magnetic fields for Sample A (upper panel) and Sample B (lower panel). The curves are measured values and the symbols are calculated based on an analysis procedure described in the text. For clarification we showed only the calculated data at 900 G for Sample B. Inset (a) presents $T_c(\theta)$ at 1 T for Sample A, demonstrating the failure of the scaling at low T ($< T^*$). Inset (b) shows comparisons of $T_c(\theta)$ data from Sample B and the reference film measured at $H = 900$ G.

the superconducting transition temperature anisotropy has been dramatically altered by the hole-array. Comparison of Samples A and B in Fig.2 also shows that the periodicity in $T_c(\theta)$ changes with hole-hole separation distance. We show below that these oscillations in tilted fields arise from Little-Parks fluxoid quantization by the hole-array and that the smooth background arises from 1D flux confinement in the sections between the holes. Both features are quantitatively described on their entirety by experimentally determined scaling laws.

In a regular square superconducting wire network where the width of the sections between neighboring square holes is of the order of the superconducting coher-

ence length, fluxoid quantization in perpendicular fields causes Little-Parks oscillations to appear in the field dependence of the critical temperature $T_c(H)$[9]. Here, the kinetic energy of strong shielding currents required to maintain fluxoid quantization in the holes lowers the superconducting condensation energy and depresses the critical temperature. The period of the oscillation reflects the applied field required to add an additional flux quantum into each hole in the array, as described by Pannetier *et. al.*[9]. The $T_c(H_\perp)$ phase diagram for perpendicular fields in Fig.3a for Sample A show similar oscillations with a period in field of 1070 ± 50 G, consistent with the calculated value of $H_{1\perp} = 1062$ G at which each hole traps a single flux quantum. Furthermore, the oscillatory component $\Delta T_c(H_\perp)$ in the $T_c(H_\perp)$ curve generally follows a smooth upper-bound background curve (green solid line in Fig.3a), similar to that observed in a superconducting aluminum wire network[9], suggestive of the Little-Parks effect. The smooth background curve in $T_c(H_\perp)$ without the Little-Parks oscillations follows a parabolic relationship[9,36] and can be derived by scaling $T_c(H_\parallel)$ at $\theta = 90°$ where in this geometry, the applied field has no perpendicular component to induce additional T_c suppression[37]. As shown in Fig.3a, the $T_c(H_\parallel)$ curve indeed forms a nearly perfect upper-bound for $T_c(H_\perp)$ curve after multiplying $H_\parallel$ with a scaling factor of $\alpha_\perp = 0.587$. By numerically subtracting this upper-bound parabolic background from the experimental $T_c(H_\perp)$ curve, we can obtain the Little-Parks effect induced oscillatory T_c suppression $\Delta T_c(H_\perp)$ which is shown in the inset of Fig.3a. The maximum $\Delta T_c(H_\perp) \approx -28$ mK is very close to the theoretical value $\Delta T_c = -0.18\xi_0 l T_{c0}/R^2 = -26$ mK for a thin Nb ring of radius $R = 75$ nm in the dirty limit[15], where $\xi_0 = 38$ nm and $l = 3.6$ nm were chosen for the calculation[16]. The decay in the amplitude of $\Delta T_c(H_\perp)$ with increasing magnetic field may originate from the slight imperfections in the arrangement of the holes in the triangular lattice[38] and/or the finite width of the circulating supercurrent path[39,40].

As the field is tilted away from the film normal, the oscillation period in $T_c(H)$ continuously increases, as demonstrated by the data in Fig.3b. Quantitatively, it follows the relationship $H_{1\theta} = H_{1\perp}/\cos\theta$, as illustrated by the solid line in the inset of Fig.3b where $H_{1\perp}$ is the oscillation period in perpendicular orietation. This angular dependence implies that the oscillations in tilted magnetic fields respond only to the perpendicular component of the applied field. Such a behavior is a consequence of the thin film geometry of the hole-array where the shielding currents are prohibited from having a perpendicular component. Consequently, a field H applied at angle of θ will cause the same ΔT_c as a field of $H\cos\theta$ applied at 0°. That is, $\Delta T_c(\theta)$ at any angle θ at a fixed magnetic field H can be the derived from $\Delta T_c(H_\perp)$ by converting $H_\perp$ to θ through a relationship $\theta = \arccos(H_\perp/H)$. The data for $\Delta T_c(\theta)$ at $H = 2500$ G are presented in Fig.4a (red open circles) as an example. It is evident that the oscillation

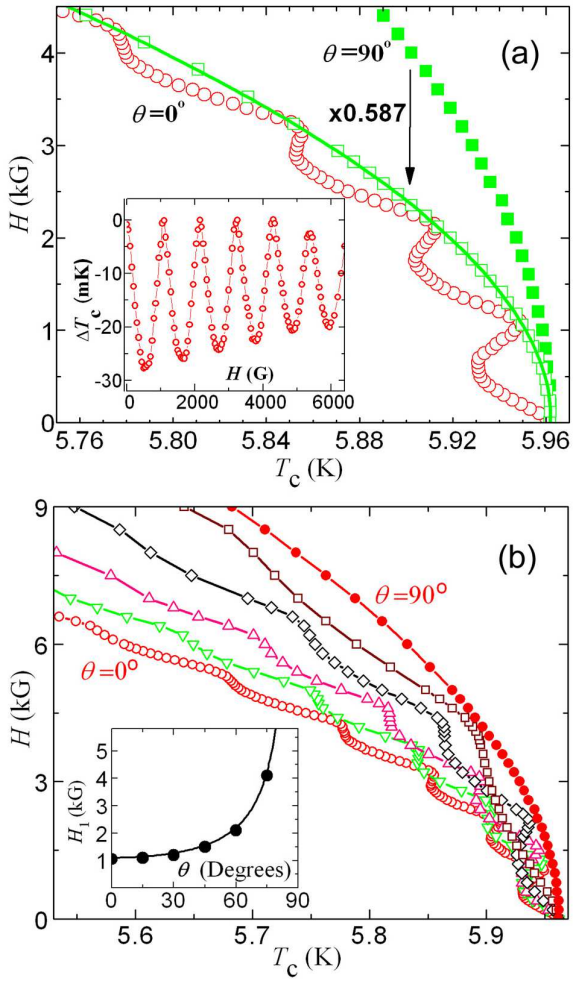

FIG. 3. (Color online) (a) $T_c(H)$ data of Sample A for $\theta = 0°$ (open circles) and 90° (solid squares). The open squares delineates a upper-bound for the $T_c(H_\perp)$ curve and was obtained by multiplying the $H_\parallel$ values with a scaling factor of 0.587. The green line represents the 1D fit to this upper-bound background data. Inset shows $\Delta T_c(H_\perp)$ by subtracting the green line from the experimental $T_c(H_\perp)$ curve. (b) $T_c(H)$ data for $\theta = 0°$, 30°, 45°, 60°, 75°, and 90° for Sample A. The inset shows the angular dependence of the oscillation period H_1.

of the calculated $\Delta T_c(\theta)$ is consistent with that of the measured $T_c(\theta)$ at the same field. That is, the oscillation in $T_c(\theta)$ comes from that in $T_c(H_\perp)$.

Following the procedure to derive the upper-bound background curve in the $T_c(H_\perp)$ (Fig.3a), we obtained an angle dependent scaling factor which is plotted in the inset to Fig.4b for both Samples A and B. Since the scaling factor α_θ is in fact the ratio of the critical field at θ ($H_{c\theta}$) and that at 90° ($H_{c\parallel}$) of the film in the absence of the influence of the holes, we first attempted to understand this anisotropy with Tinkhams 2D thin film formula[15] which now can be rewritten in terms of the scaling factor α as: $\alpha_\theta \cos\theta/\alpha_\perp + [\alpha_\theta \sin\theta/\alpha_\parallel]^2 = 1$ with $\alpha_\theta = H_{c\theta}/H_{c\parallel}$, $\alpha_\perp = H_{c\perp}/H_{c\parallel}$, and $\alpha_\parallel = 1$. This derived α_θ should have a cusp at $\theta = 90°$, in contrast

to the rounded behavior at $\theta = 90°$ shown in the experimental data in the inset of Fig.4b. Hence with this formula, we see a significant deviation from our Sample A data as indicated by the red dashed line (inset of Fig.4b), demonstrating that the anisotropy of our patterned film differs from that of a continuous film even without the consideration of the oscillations. Instead, the background anisotropy follows that of a 1D strip[35], $H_{c\theta} = H_{c\perp}(\cos^2\theta + \gamma^{-2}\sin^2\theta)^{-1/2}$ with $\gamma = H_{c\parallel}/H_{c\perp}$. Rewriting this dependence in terms of the scaling factor α yields $\alpha_\theta = \alpha_\perp(\cos^2\theta + \alpha_\perp^2\sin^2\theta)^{-1/2}$ which fits the observed scaling factors very well. This implies that a patterned superconducting film displays the critical field anisotropy of a 1D strip if the contribution from the Little-Parks effect is excluded. The quality of the fit from the scaling analysis for all fields, temperatures and angles is shown in the main panel of Fig.4b where the data are plotted as H/α vs T_c. It shows that the experimental curve at $\theta = 90°$, when properly scaled for 1D confinement, universally accounts the backgrounds for all data at all angles.

The 1D confinement is understandable in terms of the transverse dimensions of the narrowest sections between neighboring holes. These sections are confined in both thickness t and width $w \approx D - d$, similar to that in a 1D strip, although the width varies slightly due to the configuration of the circular hole. As discussed in the introduction, the critical field of a superconductor can be size-dependent if its dimensions are smaller than $\lambda(T)$. Since $\xi(T) < \lambda(T)$ in Nb, $\xi(T)$ is the characteristic length to define the confinement. In our experimental temperature range both w and t are comparable to the coherence length $\xi(T)$ as indicated by the temperatures T^* (given in Table I) above which both w and t are less than the 1D criterion of $1.84\xi(T)$[39]. This leads to the calculated $\alpha_\perp (= H_{c\perp}/H_{c\parallel} = t/w)$ to be consistent with the experimental values. The dependence of the 1D confinement on the hole configuration is also confirmed by comparing Samples A and B, where the hole separation (and therefore the confinement length) differs by approximately a factor of two.

The 1D scaling of the background anisotropy in $T_c(H)$ allows us to calculate the background curves in $T_c(\theta)$[41]. As an example, the solid line in Fig.4a presents the derived background curve for $T_c(\theta)$ obtained at $H = 2500$ G. Adding this 1D anisotropy background to the oscillatory component $\Delta T_c(\theta)$ (red open circles) gives the sum (blue open circles). The same procedure was used to produce the comparison of the calculated and experimental full phase boundary curves for Samples A and B as a function of angle shown in Fig.2. A remarkably good fit is obtained using the combination of the 1D anisotropy and the Little-Parks oscillation governed by the perpendicular magnetic field.

In conclusion, the superconducting phase boundary of a superconducting thin film with a triangular array of holes in the presence of a magnetic field displays strong anisotropy consisting of two parts: an oscillatory

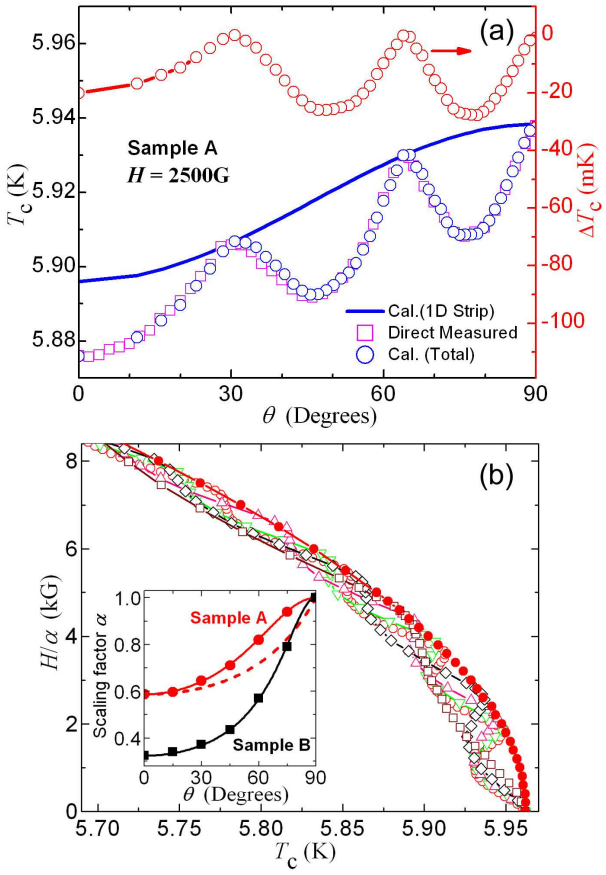

FIG. 4. (Color online) (a) Angle dependence of $T_c(\theta)$ and $\Delta T_c(\theta)$ obtained in a magnetic field of 2500 G: the red circles represent $\Delta T_c(\theta)$ derived from $\Delta T_c(H_\perp)$ by converting $H_\perp$ to θ through a relation $\theta = \arccos(H_\perp/H)$; the blue curve represents the calculated $T_c(\theta)$ curve without the hole-contribution; the blue circles are the sum of the red circles and the blue curve while the open purple squares are the experimentally measured values. (b) Scaling behavior of the $T_c(H)$ data in Fig.3b (the same symbols). Inset shows the angular dependence of the scaling factor and fits with formulas for thin film (dashed line) and 1D strip (solid lines).

Little-Parks depression of the critical temperature and a smooth background. Quantitative analysis shows that the Little-Parks oscillations respond only to the perpendicular component of the magnetic field, reflecting the in-plane nature of supercurrent circulating the holes. The smooth background differs from the expected 2D confinement expressed by the Tinkham thin film formula. Instead, it arises from 1D confinement of the superconductor to the lateral regions between neighboring holes and is fully determined by the hole configuration. The smooth background can be obtained from the experimental parallel field phase boundary using a scaling factor whose anisotropy follows the 1D confinement form.

ACKNOWLEDGMENTS

This work was supported by DOE BES under Contract No. DE-AC02-06CH11357 which also funds Argonnes Center for Nanoscale Materials (CNM) and Electron Microscopy Center (EMC) where the nanopatterning and morphological analysis were performed. ZLX acknowledges DOE BES Grant No. DE-FG02-06ER46334 (sample fabrication and imaging).

* xiao@anl.gov or zxiao@niu.edu

[1] Y. Liu, Y. Zadorozhny, M. M. Rosario, B. Y. Rock, P. T. Carrigan, and H. Wang, Science **294**, 2332 (2001).

[2] Z. Hens, D. Vanmaekelbergh, E. S. Kooij, H. Wormeester, G. Allan, and C. Delerue, Phys. Rev. Lett. **92**, 026808 (2004).

[3] Z. Wu, J. B. Neaton, and J. C. Grossman, Phys. Rev. Lett. **100**, 246804 (2008).

[4] Y. Chen, S. D. Snyder, and A. M. Goldman, Phys. Rev. Lett. **103**, 127002 (2009).

[5] I. Sochnikov, A. Shaulov, Y. Yeshurun, G. Logvenov, and I. Bozovic, Nature Nano **5**, 516 (2010).

[6] G. R. Berdiyorov, M. V. Milošević, M. L. Latimer, Z. L. Xiao, W. K. Kwok, and F. M. Peeters, Phys. Rev. Lett. **109**, 057004 (2012).

[7] J. S. Lehtinen, K. Zakharov, and K. Y. Arutyunov, Phys. Rev. Lett. **109**, 187001 (2012).

[8] R. D. Parks and W. A. Little, Phys. Rev. **133**, A97 (1964).

[9] B. Pannetier, J. Chaussy, R. Rammal, and J. C. Villegier, Phys. Rev. Lett. **53**, 1845 (1984).

[10] F. Carillo, G. Papari, D. Stornaiuolo, D. Born, D. Montemurro, P. Pingue, F. Beltram, and F. Tafuri, Phys. Rev. B **81**, 054505 (2010).

[11] A. V. Samokhvalov, A. S. Mel'nikov, J.-P. Ader, and A. I. Buzdin, Phys. Rev. B **79**, 174502 (2009).

[12] A. Y. Aladyshkin, D. A. Ryzhov, A. V. Samokhvalov, D. A. Savinov, A. S. Mel'nikov, and V. V. Moshchalkov, Phys. Rev. B **75**, 184519 (2007).

[13] I. Sternfeld, R. Koret, H. Shtrikman, A. Tsukernik, M. Karpovski, and A. Palevski, Physica (Amsterdam) **468C**, 337 (2008).

[14] M. Tinkham, Phys. Rev. **129**, 2413 (1963).

[15] M. Tinkham, *Introduction to superconductivity* (McGraw-Hill, Inc., New York,, 1996).

[16] U. Welp, Z. L. Xiao, J. S. Jiang, V. K. Vlasko-Vlasov, S. D. Bader, G. W. Crabtree, J. Liang, H. Chik, and J. M. Xu, Phys. Rev. B **66**, 212507 (2002).

[17] A. V. Silhanek, S. Raedts, M. J. Van Bael, and V. V. Moshchalkov, Phys. Rev. B **70**, 054515 (2004).

[18] S. Avci, Z. L. Xiao, J. Hua, A. Imre, R. Divan, J. Pearson, U. Welp, W. K. Kwok, and G. W. Crabtree, Appl. Phys. Lett. **97**, 042511 (2010).

[19] C. Chiliotte, G. Pasquini, V. Bekeris, J. E. Villegas, C. P. Li, and I. K. Schuller, Supercond. Sci. Technol. **24**, 065008 (2011).

[20] M. L. Latimer, G. R. Berdiyorov, Z. L. Xiao, W. K. Kwok, and F. M. Peeters, Phys. Rev. B **85**, 012505 (2012).

[21] X. S. Ling, H. J. Lezec, M. J. Higgins, J. S. Tsai, J. Fujita, H. Numata, Y. Nakamura, Y. Ochiai, C. Tang, P. M. Chaikin, and S. Bhattacharya, Phys. Rev. Lett. **76**, 2989 (1996).

[22] C. Reichhardt, C. J. Olson, and F. Nori, Phys. Rev. Lett. **78**, 2648 (1997).

[23] C. Reichhardt, C. J. Olson, and M. B. Hastings, Phys. Rev. Lett. **89**, 024101 (2002).

[24] G. R. Berdiyorov, M. V. Milošević, and F. M. Peeters, Phys. Rev. Lett. **96**, 207001 (2006).

[25] F. Yu, N. E. Israeloff, A. M. Goldman, and R. Bojko, Phys. Rev. Lett. **68**, 2535 (1992).

[26] L. Horng, J. C. Wu, T. C. Wu, and S. F. Lee, J. Appl. Phys. **91**, 8510 (2002).

[27] L. Van Look, B. Y. Zhu, R. Jonckheere, B. R. Zhao, Z. X. Zhao, and V. V. Moshchalkov, Phys. Rev. B **66**, 214511 (2002).

[28] M. Kemmler, C. Gürlich, A. Sterck, H. Pöhler, M. Neuhaus, M. Siegel, R. Kleiner, and D. Koelle, Phys. Rev. Lett. **97**, 147003 (2006).

[29] S. Tacchi, M. Madami, G. Gubbiotti, G. Carlotti, A. Adeyeye, S. Neusser, B. Botters, and D. Grundler, IEEE Trans. Magn. **46**, 1440 (2010).

[30] O. Gunawan, T. Gokmen, Y. P. Shkolnikov, E. P. De Poortere, and M. Shayegan, Phys. Rev. Lett. **100**, 036602 (2008).

[31] G. Strijkers, F. Yang, D. Reich, C. Chien, P. Searson, Y. Streiniker, and D. Bergman, IEEE Trans. Magn. **37**, 2067 (2001).

[32] T. Schneider, A. A. Serga, B. Leven, B. Hillebrands, R. L. Stamps, and M. P. Kostylev, Appl. Phys. Lett. **92**, 022505 (2008).

[33] S. Neusser, G. Duerr, H. G. Bauer, S. Tacchi, M. Madami, G. Woltersdorf, G. Gubbiotti, C. H. Back, and D. Grundler, Phys. Rev. Lett. **105**, 067208 (2010).

[34] T. G. Pedersen, C. Flindt, J. Pedersen, N. A. Mortensen, A.-P. Jauho, and K. Pedersen, Phys. Rev. Lett. **100**, 136804 (2008).

[35] J. Hua, Z. L. Xiao, A. Imre, S. H. Yu, U. Patel, L. E. Ocola, R. Divan, A. Koshelev, J. Pearson, U. Welp, and W. K. Kwok, Phys. Rev. Lett. **101**, 077003 (2008).

[36] V. V. Moshchalkov, L. Gielen, C. Strunk, R. Jonckheere, X. Qiu, C. Vanhaesendonck, and Y. Bruynseraede, Nature **373**, 319 (1995).

[37] U. Patel, Z. L. Xiao, J. Hua, T. Xu, D. Rosenmann, V. Novosad, J. Pearson, U. Welp, W. K. Kwok, and G. W. Crabtree, Phys. Rev. B **76**, 020508 (2007).

[38] M. G. Forrester, H. J. Lee, M. Tinkham, and C. J. Lobb, Phys. Rev. B **37**, 5966 (1988).

[39] M. Morelle, D. S. Golubovic, and V. V. Moshchalkov, Phys. Rev. B **70**, 144528 (2004).

[40] V. H. Dao and L. F. Chibotaru, Phys. Rev. B **79**, 134524 (2009).

[41] See Supplementary Material at [URL will be inserted by publisher] for $T_c(H)$ phase boundaries defined with various resistive criteria and Procedure to obtain the T_c anisotropy of the 1D background.